Original

Generation of novel *Il2rg*-knockout mice with clustered regularly interspaced short palindromic repeats (CRISPR) and Cas9

Suvd BYAMBAA[1)], Hideki UOSAKI[1,2)], Hiromasa HARA[1,2)], Yasumitsu NAGAO[2,3)], Tomoyuki ABE[1,2)], Hiroaki SHIBATA[1,2)], Osamu NUREKI[4)], Tsukasa OHMORI[5)] and Yutaka HANAZONO[1,2)]

[1)]*Division of Regenerative Medicine, Center for Molecular Medicine, Jichi Medical University, 3311-1 Yakushiji, Shimotsuke-shi, Tochigi 329-0498, Japan*
[2)]*Center for Development of Advanced Medical Technology, Jichi Medical University, 3311-1 Yakushiji, Shimotsuke-shi, Tochigi 329-0498, Japan*
[3)]*Center for Experimental Medicine, Jichi Medical University, 3311-1 Yakushiji, Shimotsuke-shi, Tochigi 329-0498, Japan*
[4)]*Department of Biological Sciences, Graduate School of Science, The University of Tokyo, 2-11-16 Yayoi, Bunkyo-ku, Tokyo 113-0032, Japan*
[5)]*Department of Biochemistry, Jichi Medical University, 3311-1 Yakushiji, Shimotsuke-shi, Tochigi 329-0498, Japan*

Abstract: X-linked severe combined immunodeficiency (X-SCID) is an inherited genetic disorder. A majority of X-SCID subjects carries point mutations in the Interleukin-2 receptor gamma chain (*IL2RG*) gene. In contrast, *Il2rg*-knockout mice recapitulating X-SCID phenotype lack a large part of *Il2rg* instead of point mutations. In this study, we generated novel X-SCID mouse strains with small insertion and deletion (InDel) mutations in *Il2rg* by using clustered regularly interspaced short palindromic repeats (CRISPR)/Cas9. To this end, we injected *Streptococcus pyogenes* Cas9 (SpCas9) mRNA and single guide RNA targeting the exon 2, 3 or 4 of *Il2rg* into mouse zygotes. In the F0 generation, we obtained 35 pups and 25 out of them were positive for Surveyor assay, and most of mutants displayed dramatic reductions of T and B lymphocytes in the peripheral blood. By amplicon sequencing, 15 out of 31 founder mice were determined as monoallelic mutants with possible minor mosaicisms while 10 mice were mosaic. Finally, we established new strains with 7-nucleotide deletion and 1-nucleotide insertions in the exon 2 and the exons 3 and 4, respectively. Although no IL2RG protein was detected on T cells of exons 3 and 4 mutants, IL2RG protein was unexpectedly detected in the exon 2 mutants. These data indicated that CRISPR/Cas9 targeting *Il2rg* causes InDel mutations effectively and generates genetically X-SCID mice. Genetic mutations, however, did not necessarily grant phenotypical alteration, which requires an intensive analysis after establishing a strain to confirm their phenotypes.

Key words: animal model, clustered regularly interspaced short palindromic repeats (CRISPR)/Cas9, genome-editing, *Il2rg*, X-linked severe combined immunodeficiency (X-SCID)

Introduction

The interleukin-2 receptor γ chain (IL2RG), encoded from chromosome X, is an essential common receptor for IL-2, 4, 7, 9, 15 and 21 [3, 21] and plays an vital role in lymphoid-lineage cell development through activation of Janus kinase 3 [11, 20]. Mutations in *IL2RG* gene, causing the truncation or altered amino sequence of the protein, impair the interaction of the receptor complexes to cytokines, and as a result, the differentiation of T and natural killer (NK) cells is blocked [4]. Allogeneic transplantation of hematopoietic stem cells (HSCs) is

the first-line treatment of X-SCID [4]. Gene therapy, autologous transplantation of HSCs introduced with *IL2RG* gene by retro- or lentiviral vectors, is another therapy in clinical trials [13]. However, due to limited availability of HLA-matched donors and leukemia caused by the insertional mutagenesis of the viral vector [14], another alternative therapy might be required. With recent advances in targeted gene correction using designed nucleases [2], autologous transplantation of gene-corrected HSCs is one alternative and promising method for X-SCID treatment.

To develop genome-editing therapy, a better murine model of X-SCID is preferred. Nearly 200 types of mutations causing X-SCID have been reported and they occur in any of eight exons, mainly as point or frameshift mutations [29]. In contrast, current murine models of X-SCID are either deletion of exon 3 and entire exon 4–8 [3] or two-third of the exon 7, the intron 7 and the half of exon 8 of *Il2rg* [27]. The mice with the loss-of-function mutations of *Il2rg* are without functional T, B and NK cells and are good models for gene therapies. However, as the nature of the mutations, they are not suitable for the disease model of genome-editing therapies. Therefore, *Il2rg*-knockout mice with small insertion or deletion (InDel) mutations are awaited.

Genetically engineered mouse models with site-specific transgene insertion, gene replacement or conditional knock-out alleles were mostly generated through a homologous recombination in embryonic stem (ES) cells. In contrast, clustered regularly interspaced short palindromic repeats (CRISPR) and CRISPR-associated protein 9 (Cas9) allows direct generation of targeted genome-edited animals due to high efficiency of genome editing [8, 10, 35]. More importantly, CRISPR/Cas9 enable to generate an animal model with small mutations efficiently [18].

In this study, we developed novel *Il2rg*-knockout mouse strains that have short InDel mutations in exons 2, 3 or 4 by CRISPR/Cas9.

Materials and Methods

Animals

C57BL/6J and Multi Cross Hybrid ICR (MCH [ICR]) mice were purchased from SLC Japan (Shizuoka, Japan) and CLEA Japan (Tokyo, Japan), respectively. All mice were housed at Center for Experimental Medicine, Jichi Medical University. All animal experiments reported here were approved by the Institutional Animal Care and Concern Committee at Jichi Medical University. Animal care and all experiments were performed in accordance with the committee's guidelines.

Designing and preparing guide RNA

The guide sequences of guide RNAs (gRNAs) for generating *Il2rg*-knockout mice were designed in exon 2 (AGCGTGAGGTTGGTTGCCTG), exon 3 (ACAAAT-AGTGACTGCACTCC) or exon 4 (TTAGATTTTCTG-GAGCCCGT) of *Il2rg*. All gRNA sequences were designed using online software, Benchling (https://benchling.com). Their specificities (off-target scores and potential off-target sites) and potential on-target efficiencies (on-target scores) were also examined with Geneious 11.1.5 (GRCm38.p4 for mouse chromosome dataset) (Biomatters Ltd., Auckland, New Zealand), CCTop, Cas-OFFinder and CRISPRdirect [1, 25, 32]. We calculated off-target scores using Geneious R11. For the calculation, we used mouse genomic DNA sequences, GRCm38.p4, with allowing maximum three mismatches and one indel to the off-target sites[17]. To generate single guide RNAs (sgRNAs) for *Il2rg* exon 2, 3 and 4, GeneArt Precision gRNA Synthesis kit (Thermo Fisher Scientific, Waltham, MA, USA) was used, followed by *in vitro* transcription (IVT) with CUGA3/CUGA7 (Nippon Gene Tech., Tokyo, Japan) as following manufactures' instructions. Briefly, we assembled T7 promoter, the target-specific sequences and trans-activating CRISPR RNA (tracrRNA) fragment to generate the DNA template for IVT. The oligonucleotides for the T7 promoter and the target-specific sequences were synthesized as follows; *Il2rg* exon2: fwd; TAATACGACTCACTATAG-AGCGTGAGGTTG-GTTG, rev; TTCTAGCTCTAAAAC-CAGGCAACC-AACCTCACGC; *Il2rg* exon3: fwd; TAATACGAC-TCACTATAG-ACAAATAGTGACTGCA, rev; TTCTAGCTCTAAAAC GGAGTGCAGTCACTATTTG, *Il2rg* exon4: fwd; TAATACGACTCACTATAG-TTA-GATTTTCTGGAGC; rev; TTCTAGCTCTAAAAC-ACGGGCTCCAGAAAATCTA. Then, IVT reactions were performed using CUGA3/CUGA7. After IVT, the template DNA were removed by 1U/μl DNase I digestion. Finally, sgRNAs were purified with phenol/chloroform extraction, and the quality of the RNA was assessed by gel electrophoresis using 2% agarose gel with 3-(N-morpholino) propanesulfonic acid (MOPS) buffer and 37% formaldehyde.

Co-injection of Cas9 mRNA and gRNA into pronucleus in zygotes

20 ng/μl *Streptococcus pyogenesis* Cas9 (SpCas9) mRNA (Thermo Fisher Scientific) and 5 ng/μl sgRNAs targeting exon 2, 3 or 4 of mouse *Il2rg* were microinjected into pronucleus of zygotes. Microinjected zygotes were transferred into pseudopregnant MCH (ICR) mice at the one- or two-cell stage and founders were delivered by Caesarian section.

Surveyor assay and DNA sequencing for target sites

The genomic DNA was extracted from the peripheral blood or tail-cut tissues with the DNA extraction kit (Qiagen, Venlo, Netherlands) and CRISPR/Cas9-mediated genomic mutations were detected with the Surveyor mutation detection kit (Integrated DNA Technologies, Skokie, IL, USA). The target site of *Il2rg* exon 2 to 4 was amplified with ExTaq DNA polymerase (Takara Bio, Otsu, Japan) and the primer set 5'-AGATCC-TTCTTAGTCCTTCAGCTGCT-3' and 3'-GCTTGG-CCTTAGCCACTGC-5'. Heteroduplex was formed under the denaturing and re-annealing protocol with a thermal cycler as indicated in the manufacturer's instructions. Then, the samples were treated with Surveyor nuclease and the DNA fragments were analyzed by agarose gel electrophoresis and by MultiNA, a microchip electrophoresis system (Shimadzu, Tokyo, Japan) with DNA-12000 Reagent Kit (Shimadzu, Tokyo, Japan).

To analyze the introduced mutations, Sanger DNA sequencing was performed in all mutated F1 female mice. The peripheral blood was obtained from all F1 mice, and DNA was extracted using the DNA extraction kit. PCR fragments of the targeted sites were amplified and then cloned to the pTAC-2 vector (Biodynamics, Tokyo, Japan). After transformation to One Shot Stbl3 Chemically Competent *E. coli*(Thermo Fisher Scientific), four clones were collected for each mouse. Plasmids were extracted by the Qiaprep Spin Miniprep kit (Qiagen, Hilden, Germany) for DNA sequencing.

Amplicon sequence

To precisely examine the mosaicisms in the founder lines, we performed amplicon sequencing. We first amplified exon 2–4 of *Il2rg* using the primer set described above, then performed nested PCR to amplify each exon using primer pairs (*Il2rg* Ex2: 5'-TCTACAGCCCCT-GAACACCT-3', 3'-CAGTCTCTCCCAGCTAACCTC-CCT-5'; *Il2rg* Ex3: 5'-TGGCCCATCATTCTTTTG-CCTTG-3', 5'-CTGTACAGCTCGCCTCTGG-3'; *Il2rg* Ex4: 5'-CTCCAAGATCCTGACTTGTCTAGGC-3', 3'-GTCCAGCTTCGATCTCTGTTGCT-5'). Illumina sequence adapters and indices (SeqCap Adapter Kit A, Roche, Basel, Switzerland) were ligated using KAPA LTP Library Preparation Kit (KAPA Biosystems, Wilmington, MA, USA). Pooled library was sequenced with MiSeq v2 Nano, 150-bp, paired-end (Illumina, San Diego, CA, USA). As we pooled 33 samples with only 12 indices (ones from each exon line were assigned to one index), we demultiplex based on the sequence results using R package ShortRead [24]. Low coverage mutants were excluded from the analysis (Ex3 #7 and 9). The

mutations in each founder line were examined and mosaicisms were calculated for each mutation using R package amplican[22] with the demultiplexed, full-length and paired-end sequences. In some cases, amplican counted reads separately if reads contain some PCR or sequence errors. Therefore, we further examined the mosaicisms only at the target site sequences (Figs. 3B and C) after merging the paired-end sequences with Paired-End reAd mergeR (PEAR) [34].

Flow cytometry

The peripheral blood was obtained through the jugular vein of mice and mononuclear cells were isolated through erythrocyte lysis. The cells were stained with anti-mCD45-FITC, anti-CD45.2-BV711 (BD Bioscience, East Rutherford, NJ, USA), anti-CD3-PE, anti-CD3-APC, anti-CD19-PE/Cy7, anti-CD11b-BV421 and anti-Gr-1-BV510 (BioLegend, San Diego, CA, USA) to identify lymphoid and myeloid lineages of cells. Anti-CD132-PE (clone TUGm2, BioLegend) was used to detect IL2RG protein. Flow cytometry was performed with BD LSR Fortessa II, The BD FACS Aria Fusion (BD Bioscience).

Results

In this study, we selected gRNA for exons 2, 3 and 4 of *Il2rg* with at least 90% off-target score and higher on-target score (Fig. 1A). SpCas9 mRNA and gRNA targeting exons 2, 3 or 4 of *Il2rg* were injected into mouse zygotes (Fig. 1B, Table 1). To identify mutated founders, we performed genotyping and phenotyping for all F0 founders by Surveyor assay and flow cytometry, respectively (Figs. 1C and 2A–G). In the F0 generation, we obtained 35 offspring (14, 12 and 9 mice for exons 2, 3 and 4, respectively) (Table 1). Among them, 29 were positive for the Surveyor assay (71–92%) (Figs. 2A, C and E). We confirmed dramatic reductions of T and B lymphocytes (CD3$^+$ and CD19$^+$, respectively) and the existence of granulocytes (Gr1$^+$/CD11b$^+$) in the peripheral blood of most mutated founders (Figs. 2B, D and F) and representative flow-cytometric results are shown in Fig. 2G (*Il2rg* Ex2 #2, Ex3 #1, Ex4 #5). Of note, some female mutants positive for Surveyor assay also displayed the reductions of T and B cells, indicating bi-allelic mutations (e.g. *Il2rg* Ex2 #4, #8, #11, #12 and #14), while other mutated males and females retained normal counts of T and B cells, suggesting in-frame mutations, heterozygous mutants or mosaicism (e.g. *Il2rg* Ex3 #2, #4 and #6).

To further examine mosaicisms of founder lines, we performed amplicon sequencing (Fig. 3A). Among 33
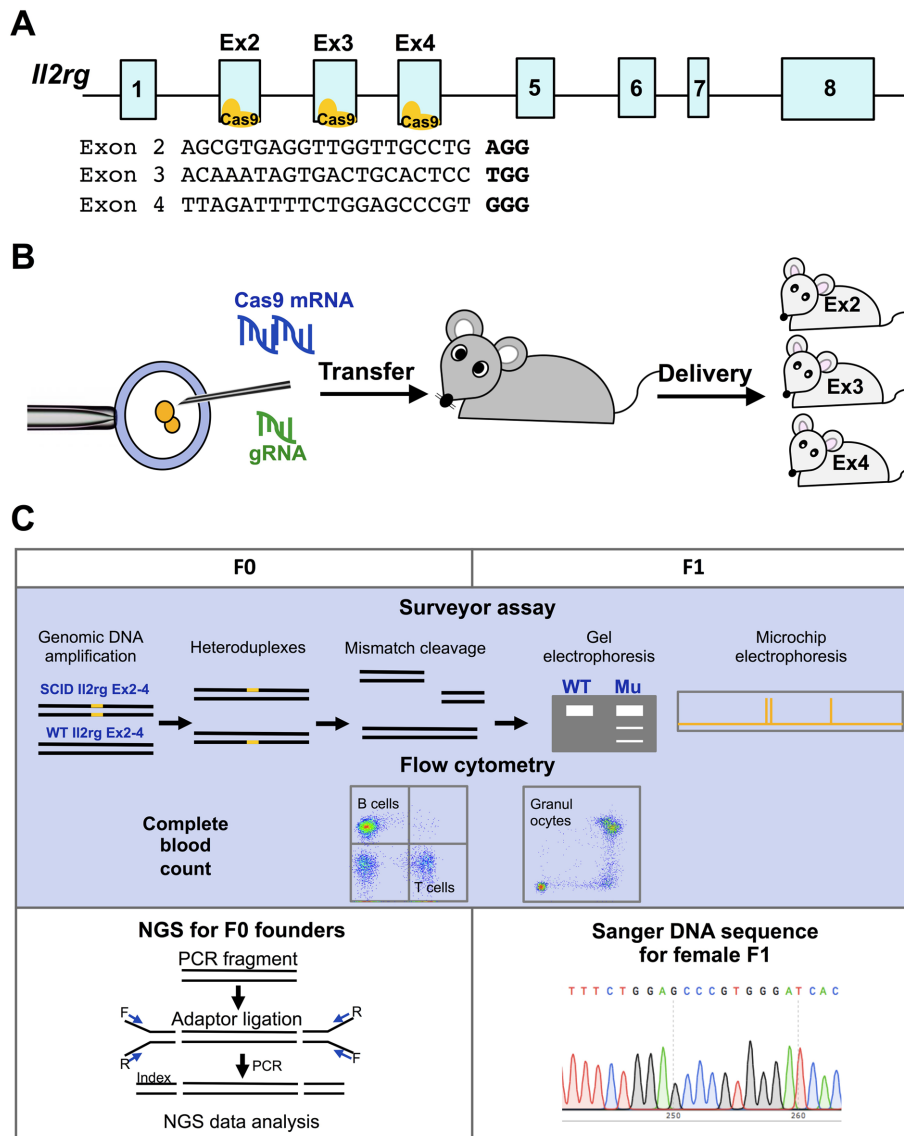
Fig. 1. Experimental design for the generation of CRISPR/Cas9-mediated X-SCID mice. (A) A schematic diagram showing the target sites of gRNAs in the *Il2rg* gene exon 2, 3 and 4. (B) A schematic presentation for generation of *Il2rg*-mutant mice by CRIPSR/Cas9. (C) Experimental design of *Il2rg*-knockout mice. For F0 and F1 generation, all of offspring were subjected to tail cut at 4 weeks after delivery for sampling and Surveyor assays were performed for genotyping. Amplicon sequencing was also performed for founder mice to determine mosaicisms. With F1 generation, Sanger DNA sequencing was performed to confirm mutations in the strains.

Table 1. Generation of founders

Target	Numbers of zygote transferred	Numbers of offspring with mutations (%)[a]		
		Total	Male	Female
Il2rg Ex2	42	10/14 (71.4%)	5/5 (100%)	5/9 (55.5%)
Il2rg Ex3	42	11/12 (91.6%)	6/7 (85.7%)	5/5 (100%)
Il2rg Ex4	16	8/9 (88.9%)	3/3 (100%)	5/6 (83.3%)

[a]Analyzed by Surveyor assay.

examined (Ex2 #6 and #7 were not examined), two were not sequenced well (Ex3 #7 and #9, <1,000 reads/sample) and excluded from the analysis. Ex3 #5 had large deletion and insertion (90% of the reads were the identical sequence, data not shown). In six mice, the wild-type sequences were identified at 96.4% in Ex2 (#10, 13), 94.5% in Ex3 (#10, 12) and 95.1% in Ex4 (#6, 8) of the reads (Fig. 3B-D), confirming the Surveyor assays (Fig. 2). Fifteen mutants (9 males and 6 females) were monoallelic with mutated sequences with minor possible mo-
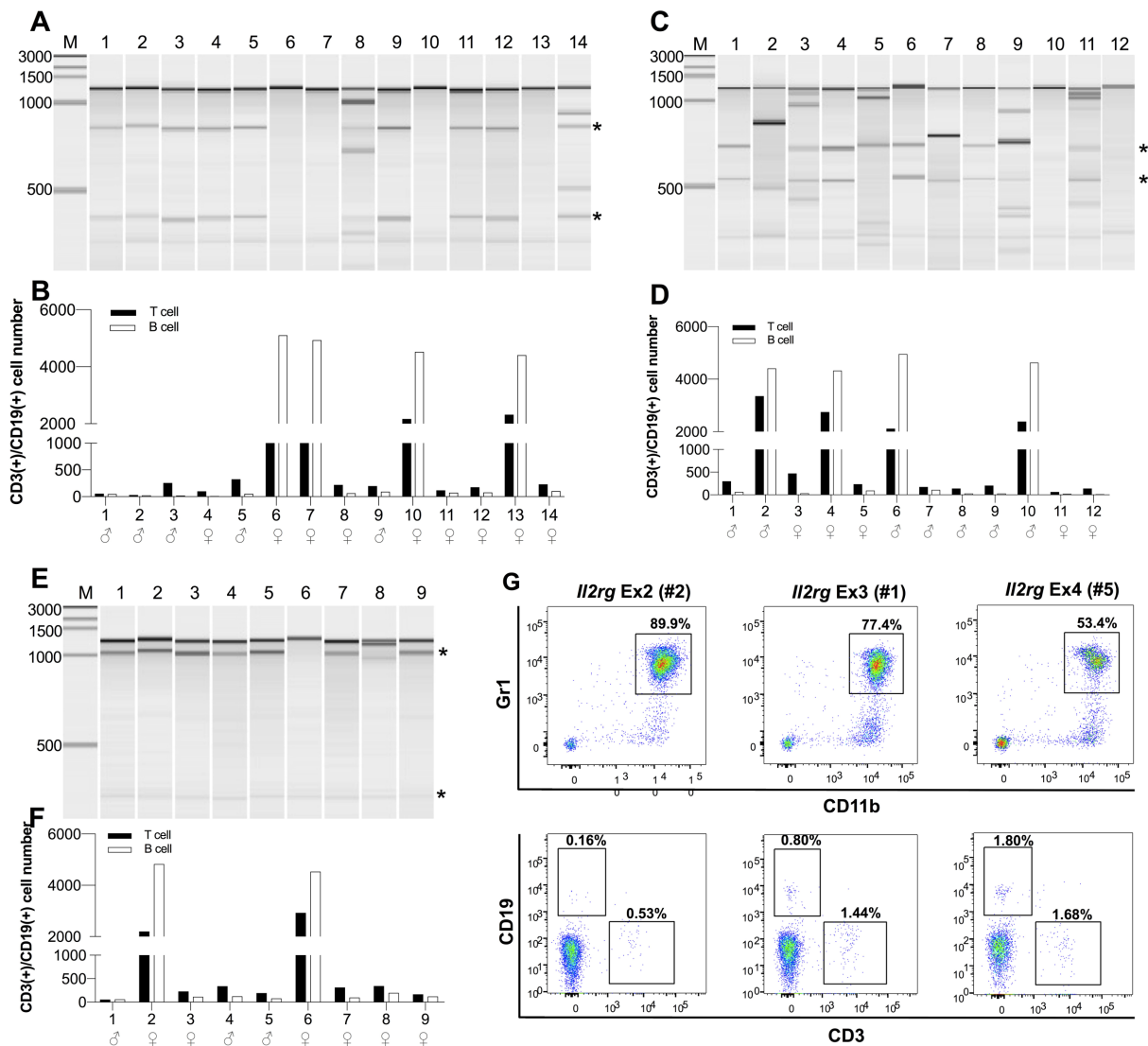
Fig. 2. Phenotypical and genotypical analysis of *Il2rg*-targeted F0 founders. Phenotyping with flow cytometry and genotyping with Surveyor assays of founder mice. (A, C, E) Electrophoresis results of Surveyor assays. Expected mutated bands are indicated with black asterisks. (B, D, F) Flow cytometry results: Black bars, the numbers of CD3^{+} T cells; white bars, the numbers of CD19^{+} B cells in the peripheral blood of the mice. (G) Representative flow cytometry results showing the reductions of T and B cells and the existence of granulocytes (Gr^{+}/CD11b^{+} cells) in the peripheral blood of *Il2rg* Ex2 #2, Ex3 #1 and Ex4 #5 mice.

saicisms (at least 90% of the reads were identical at the target sites) while 10 mutants (4 males and 6 females) were more heterogeneous with two to four different sequences detected (Figs. 3B–D). Of note, 3-nucleotide deletion in Ex3 (Ex3 #4, 6) did not alter T and B cell counts, whereas 9-nucleotide deletion in Ex4 (Ex4 #4, 7) were enough to abolish T and B cell development. Overall, mutations were in most part deletions between 2- to 14-nucleotide, 1-nucleotide substitution or 1-nucleotide insertion except one mutant with larger insertion and deletion (Figs. 3C and D, Supplementary Fig. 1). Specifically, 14-nucleotide deletion in the Ex2 was the most frequent mutation found in the Ex2 founder mice (45.5%, Fig. 3C). The target site at the Ex3 was mainly unedited (33.1%) while 1-nucleotide insertion was the

most frequent mutation (24.2%). At the Ex4, 9-nucleotide deletion was the majority of editing (32.0%). We also performed Surveyor assay for detecting possible off-target mutations. Total 24 sites were selected using CCTop and Cas-OFFinder for *Il2rg* Ex 2, 3 and 4 (Supplementary Table 1). Based on Surveyor assay, we did not observe any specific mutations in 8 potential off-target sites for Ex2 ; 9 for Ex3; and 7 for Ex4 (Supplementary Fig. 3). Taken together, the injection of Cas9 mRNA and gRNA caused mutations effectively.

To test germ-line transmission and to determine mosaicism in germ cells, we crossed one male founder from each target with the wild-type C57BL/6J female mice (Fig. 4A). In the female offspring of F1 generation, we found that total 13 out of 15 mice (87.7%) had mutated

A

First PCR

Ex2 Ex3 Ex4

Nest PCR
Amplicon sequence

ampliCan

to alignment and count the reads

Mosaicism

B

Unique reads percentage of shares

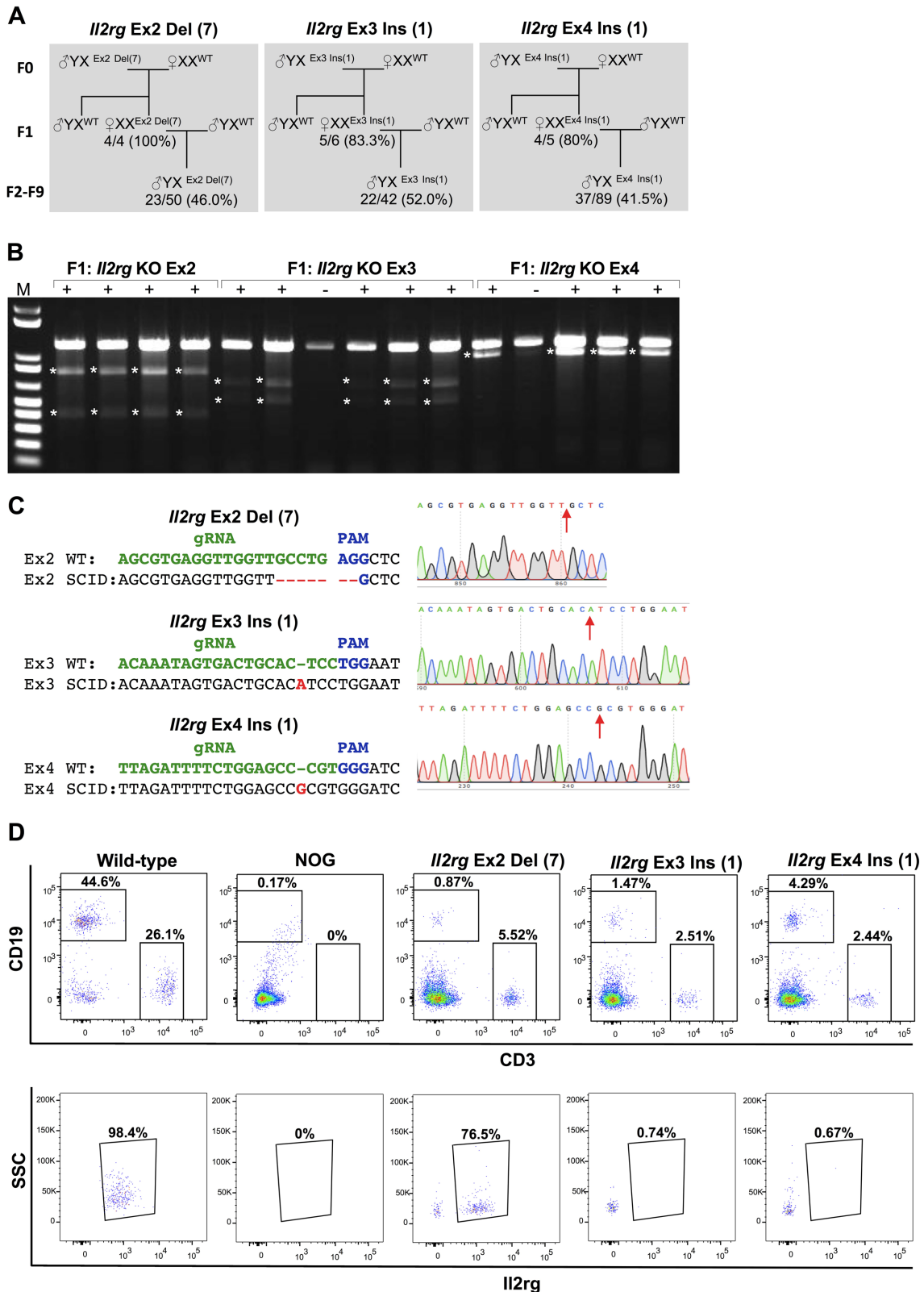| 1 2 3 4 5 8 10 11 12 13 14	1 2 3 4 6 8 10 11 12	1 2 3 4 5 6 7 8 9
Il2rg Ex2 founders	*Il2rg* Ex3 founders	*Il2rg* Ex4 founders

wild type
frequent allele 1st 2nd 3rd
others

C

Il2rg Ex2

others (3.1%)
WT (16.1%)
2bp del (2.9%)
4bp del (16.1%)
8bp del (3.3%)
7bp del (8.1%)
8bp del (5.0%)
14bp del (45.5%)

Il2rg Ex3

others (6.1%)
1bp in (24.2%)
WT (33.1%)
13bp del (8.6%)
3bp del (13.8%)
8bp del (14.3%)

Il2rg Ex4

others (5.1%)
WT (22.6%)
1bp in (19.9%)
8bp del (20.3%)
9bp del (32.0%)

D

```
Il2rg Ex2 founder
                          PAM        gRNA                      Freq
Wild type  ATAGCAGTTCTGAGCCTCAGGCAACCAACCTCACGCTGCA
      #1   ATAGCAGTTCTGAG--------------CCTCACGCTGCA        97.7%
     #2-1  ATAGCAGTTCTG--------GCAACCAACCTCACGCTGCA        60.1%
     #2-2  ATAGCAGTTCTGAGCCTCAGG--ACCAACCTCACGCTGCA        34.9%
      #3   ATAGCAGTTCTGA---------------ACCTCACGCTGCA       95.7%
      #4   ATAGCAGTTCTGAG--------------CCTCACGCTGCA        98.2%
      #5   ATAGCAGTTCTGAGCCTCA----ACCAACCTCACGCTGCA        96.5%
      #8   ATAGCAGTTCTGAG--------------CCTCACGCTGCA        98.3%
      #9   ATAGCAGTTCTGAGC-------AACCAACCTCACGCTGCA        96.6%
     #10   ATAGCAGTTCTGAGCCTCAGGCAACCAACCTCACGCTGCA        96.3%
     #11   ATAGCAGTTCTGAGCCTCA----ACCAACCTCACGCTGCA        97.1%
    #12-1  ATAGCAGTTCTGA--------------ACCTCACGCTGCA        49.8%
    #12-2  ATAGCAGTTCTGA---------------CCTCACGCTGCA        47.7%
     #13   ATAGCAGTTCTGAGCCTCAGGCAACCAACCTCACGCTGCA        96.5%
    #14-1  ATAGCAGTTCTGAG--------------CCTCACGCTGCA        38.6%
    #14-2  ATAGCAGTTCTGAGCCTCA-----CCAACCTCACGCTGCA        38.0%
    #14-3  ATAGCAGTTCTGA---------------ACCTCACGCTGCA       20.5%

Il2rg Ex3 founder
                          PAM        gRNA                      Freq
Wild type  TGATAATAATACATTCCAGGA GTGCAGTCACTATTTGTTC
      #1   TGATAATAATACATTCCAGGATGTGCAGTCACTATTTGTTC      96.8%
     #2-1  TGATAATAATACATTCCAGGA ATGCAGTCACTATTTGTTC      75.8%
     #2-2  TGATAATAATACATTCCAGGA GTGCAGTCACTATTTGTTC      21.2%
      #3   TGATAATAATACATTCCAG-- -----TCACTATTTGTTC       91.7%
     #4-1  TGATAATAATACATTCCAG-- --TCACTATTTGTTC          36.7%
     #4-2  TGATAATAATACATTC----- --------ACTATTTGTTC      33.2%
     #4-3  TGATAATAATACATTCCAG-- -TGCAGTCACTATTTGTTC       28.4%
      #6   TGATAATAATACATTCCAG-- -TGCAGTCACTATTTGTTC       95.4%
     #8-1  TGATAATAATACATTCCAGGA GTGCAGTCACTATTTGTTC       50.3%
     #8-2  TGATAATAATACATTCCAGGATGTGCAGTCACTATTTGTTC      45.3%
     #10   TGATAATAATACATTCCAGGA GTGCAGTCACTATTTGTTC       96.4%
    #11-1  TGATAATAATACATTCCAGGA GTGCAGTCACTATTTGTTC       37.9%
    #11-2  TGATAATAAT----------- --GCAGTCACTATTTGTTC      43.9%
     #12   TGATAATAATACATTCCAGGA GTGCAGTCACTATTTGTTC       92.5%

Il2rg Ex4 founder
                          PAM        gRNA                      Freq
Wild type  ATATCTCCAGTGATCCCACG GGCTCCAGAAAATCTAACAC
      #1   ATATCTCCAGTGATC----- ---TCCAGAAAATCTAACAC       96.0%
     #2-1  ATATCTCCAGTGATC----- ----CCAGAAAATCTAACAC       35.6%
     #2-2  ATATCTCCAGTGATC----- ---TCCAGAAAATCTAACAC       18.4%
     #2-3  ATATCTCCAGTGATCCCACGCGGCTCCAGAAAATCTAACAC      14.2%
     #2-4  ATATCTCCAGTGATCCCACG GGCTCCAGAAAATCTAACAC       13.7%
     #3-1  ATATCTCCAGTGATC----- ---TCCAGAAAATCTAACAC       54.4%
     #3-2  ATATCTCCAGTGATCCCACGCGGCTCCAGAAAATCTAACAC      40.7%
      #4   ATATCTCCAGTGATC----- ----CCAGAAAATCTAACAC       98.1%
      #5   ATATCTCCAGTGATCCCACGCGGCTCCAGAAAATCTAACAC      96.7%
      #6   ATATCTCCAGTGATCCCACG GGCTCCAGAAAATCTAACAC       96.4%
      #7   ATATCTCCAGTGATC----- ----CCAGAAAATCTAACAC       98.2%
      #8   ATATCTCCAGTGATCCCACG GGCTCCAGAAAATCTAACAC       93.7%
     #9-1  ATATCTCCAGTGATC----- ----CCAGAAAATCTAACAC       56.5%
     #9-2  ATATCTCCAGTGATCCCACGCGGCTCCAGAAAATCTAACAC      41.8%
```

Fig. 3. Mutation and mosaicism analysis of F0 founder lines. (A) Schematic representation of amplicon sequencing for detection of mutations and mosaicisms in the founder lines. (B) Allele frequencies in 30 founders. Blue to light blue indicate allele frequencies of up to top three and the alleles correspond to at least 10% of reads; yellow indicates the wild-type allele; gray indicates the rest of reads. (C) Detected mutation types at the each exon. Blue to light blue indicate mutation types; yellow indicates the wild-type. (D) Sequences around the target sites. The wild-type alleles of the corresponding exons were shown on the top (blue, PAM; green, gRNA; underline, potential microhomology). Sequences with at least 10% of allele frequencies in each mouse were shown (red, mutations). Freq indicates the allele frequencies of the sequence in the corresponding mouse.

alleles in the corresponding exons; that is, Ex2, 4/4 (100%); Ex3, 5/6 (83.3%); and Ex4, 4/5 (80%) (Figs. 4A and B, Supplementary Fig. 2), suggesting germline mosaicisms seems to be greater than somatic mosaicisms in the founder mice. We also performed DNA sequencing to confirm mutations in all mutated female offspring. We detected the 7-nucleotide deletion in *Il2rg* Ex2 strain and the 1-nucleotide insertion in the strains of *Il2rg* Ex3 and Ex4 (Fig. 4C), thus, we named each strain as follows: *Il2rg* Ex2 Del (7), *Il2rg* Ex3 Ins (1) and *Il2rg* Ex4 Ins (1). From F2 generation, we genotyped only male offspring. In the F2 generation, we also confirmed the dramatic reduction of T and B lymphocytes in the peripheral blood in male mice by flow cytometry (Fig. 4D). Furthermore, we obtained mutant male and heterozygote

female mice in generation F2 to F9. Overall, the mutations were carried in approximately 45.3% of male offspring by following Mendelian law (Fig. 4A).

Finally, we examined IL2RG protein expression on CD3^{+} T cells by flow cytometry (between F5 to F7 generation). Among the three strains of mice, T cells in *Il2rg* Ex2 Del (7) were positive for IL2RG protein (Fig. 4D), while T cells in two other strains (*Il2rg* Ex3 Ins (1) and *Il2rg* Ex4 Ins (1)) did not express IL2RG protein (Fig. 4D). The results show that even CRISPR/Cas9-mediated approach is highly efficient to induce targeted mutations like small InDels, some of mutations may remain inefficient to fully impair gene function.

Fig. 4. Germline transmission and the expression of Il2rg on T cells of the three strains. (A) A diagram of germ-line transmission. One male founder from each target was crossed with wild-type C57BL/6J mice. For F2 to F9 generations, total numbers of *Il2rg*-mutated male mice were indicated. (B) Surveyor assays for detecting mutations in *Il2rg* Exon 2, 3 or 4 in F1 female mice. The expected mutated bands were indicated with white asterisks. (C) Sequencing results of the new strains: a 7-nucleotide deletion in the *Il2rg* Ex2 Del (7) strain; and 1-nucleotide insertions in the strains Ex3 Ins (1) and Ex4 Ins (1) (red dash and text indicate mutations). (D) Flow cytometry of CD3, CD19 and IL2RG of the peripheral blood from C57BL/6J (wild-type), NOG and the three strains of *Il2rg*-mutated mice. Top panels show CD3 (T cells) and CD19 (B cells) of the peripheral blood. Bottom panels show IL2RG in CD3⁺ fractions from top panel. To note, almost all wild-type T cells express IL2RG, while 76.5% and less than 1% in Ex2 Del (7) and Ex 3 Ins (1) and Ex 4 (1), respectively. No T cells were detected in NOG mice.

Discussion

In this study, we generated novel strains of *Il2rg*-knockout mice by CRISPR/Cas9 mRNA injection. We proved that targeted gene disruption with CRISPR/Cas9 works effectively and provides several advantages. First, CRISPR/Cas9 can induce small mutations like small frameshift insertions or deletions that are enough to disrupt *Il2rg*. Second, *Il2rg*-knockout mice were generated within three months with high efficiency (mutation efficiencies were more than 71%). Finally, the new *Il2rg*-knockout mice were C57BL/6J background, thus no backcross was required to establish the strains.

We found CRISPR/Cas9-mediated mutations varied from 14-nucleotide deletion to one-nucleotide insertion except one with a larger InDel mutation and also found mosaicisms (15 mutants with minor mosaicisms or potentially due to PCR/sequencing error while 10 mutants with major mosaicisms) confirmed by the amplicon sequencing. Mosaicism is one of the remaining issues with CRISPR/Cas9-mediated mutagenesis. Injection and electroporation of Cas9 mRNA and gRNA are commonly used as a delivery method of CRISPR/Cas9 to zygotes [15, 28]. However, these methods induce mosaicism because the delivery is carried out at E0.5 or later while mouse first genome replication starts around E0.4 [16]. The time lag of the translation from mRNA to protein is another factor to delay the genome editing in a zygote. Recently, electroporation of Cas9 protein and gRNA into zygotes becomes a more popular method as higher quality Cas9 protein and gRNA became available. More importantly, non-mosaic animals were established by this method [7, 8, 16].

Interestingly, there were predominant types of mutations in two targets (Ex2, 14-nucleotide del; Ex4, 8- or 9-nucleotide del and 1-nucleotide ins). CRISPR/Cas9-mediated double strand breaks are mostly repaired by non-homologous end joining (NHEJ). However, in some cases, alternative NHEJ takes place called microhomology-mediated end-joining (MMEJ) [26]. At the sites of the targets, we identified potential microhomology sequences (shown as underbars in Fig. 3D). For example, around the target site of Ex2, two CCTCA were spanned by Cas9 cleavage site and the nine nucleotides in between the microhomology and one CCTCA seemed to be excised to form 14-nucleotide deletion.

One-nucleotide insertion at the exon 3 or 4 of *Il2rg* and even 9-nucleotide and in-frame deletion at the exon 4 were enough to abolish IL2RG protein expression on T cells. In contrast, the mutant mice with 7-nucleotide deletion in exon 2 carried T cells expressing IL2RG protein, which highlights the importance of an extensive analysis for newly generated mutants. Similar results were recently reported [31]. Among 193 frameshifts generated by CRISPR-Cas9, one third of induced frameshift mutations resulted in complete loss of protein expression, however one third of them still remained expressed, mostly at very low level. Moreover, choosing target exons is more important for generating phenotypically correct knockout animals. Triple-targeting CRISPR would be an option for this purpose [33]. The nature of IL2RG protein expression from the mutated *Il2rg* allele remains to be characterized. The reduction of T-cell number is obvious in the exon 2 mutants. Therefore, the IL2RG function or activity is supposed to be lower. To detect IL2RG protein, we used anti-CD132-PE (TUGm2) monoclonal antibody. The exact epitope of this antibody is unknown, but it is predicted around Lys158 of IL2RG [12]. Because all of the gRNAs used in this study are located in 5' side of Lys158, all indels equally disrupt the epitope sequence if splicing occurs in the same manner as wild-type sequence. Therefore, there might be exon skipping, alternative splicing or alternative start codon as proposed in a previous study [30]. As a signal peptide is coded in exon 1, exon skipping or alternative splicing are more likely for the expression of the altered IL2RG protein. Several studies reported that CRISPR/Cas9-mediated mutations can cause exon skipping by boundary deletion of intron and exon (3' splice site), generating new splicing donor sites or larger exon removal [30].

As noted in the introduction, the *Il2rg*-knockout mice established previously have large deletions of *Il2rg* [11, 19, 27]. In contrast, our new *Il2rg*-knockout strains have short InDel mutations, which more faithfully reflect mutations seen in X-SCID patients and thus should be preferable for developing genome-editing therapies. With the C57Bl/6J background, our strains have CD45.2+ lymphocytes while NODShi.Cg-*Prkdc*^scid^*Il2rg*^tm1Sug^ (NOG) mice have CD45.1, which allows us to perform congenic transplantation of HSCs from the new strains to NOG, or *vice versa*. In addition, due to their contract restrictions, it is not allowed to mate NOG and NOD. Cg-*Prkdc*^scid^*Il2rg*^tm1Wjl^ (NSG) mice with other strain. These features also give advantage to our new strains to develop therapeutics. Patient-derived induced pluripotent stem (iPS) cells or bone marrow samples from X-SCID patient can also be used for the models of X-SCID [5, 23]. However, it is still challenging to generate HSCs from iPS cells, and the bone marrow samples are insufficient for the demands. Needless to say, generation of disease model animals with the exactly same mutations as patients is helpful to develop clinical treatments and mouse models with patient-specific mutations such as

X-linked retinoschisis or Borjeson-Forssman-Lehmann syndrome were reported [6, 9]. However, as there are more than 200 mutations identified to cause X-SCID, it would be more complicated to select and generate each mutation to model a patient unless one specific mutation is the focus of a research. To note, though the homologous recombination (HR)-mediated targeted knock-in with single-stranded oligodeoxynucleotides (ssODNs) became more efficient, it is still less efficient than NHEJ-mediated knock-out [36]. Thus, NHEJ-mediated knock-out might be the first choice to generate a new mouse model to recapitulate disease phenotypes thus far.

In summary, we have generated three strains of *Il2rg*-knockout mice with small InDel mutations by using CRISPR/Cas9 mRNA and gRNA. The novel strains established by CRISPR/Cas9 should provide a valuable model for evaluating genome-editing therapy. It was highly effective to produce such mutations with minor mosaicisms, although a frameshift InDel mutation may not completely abolish the protein expression but just alter the function. As genome-editing therapy has gained more interest, more animal models with small mutations mimic to patients are awaited.

Author Contributions

S.B. designed experiments, performed experiments, analyzed data, prepared figures, wrote and revised a manuscript; H.U. designed experiments, performed experiments, analyzed data, wrote and revised a manuscript; H.H. designed experiments and wrote a manuscript; H.S. designed experiments and performed experiments; T.A. designed experiments; Y.N. performed experiments; O.N. generated reagents; T.O. designed experiments, performed experiments, analyzed data and wrote a manuscript, and Y.H designed experiments, analyzed data, wrote and revised a manuscript.

Conflict of Interests

All authors declare no competing financial interests in this study.

Acknowledgements

References

1. Bae, S., Park, J. and Kim, J.S. 2014. Cas-OFFinder: a fast and versatile algorithm that searches for potential off-target sites of Cas9 RNA-guided endonucleases. *Bioinformatics* 30: 1473–1475. [Medline] [CrossRef]
2. Birling, M.C., Herault, Y. and Pavlovic, G. 2017. Modeling human disease in rodents by CRISPR/Cas9 genome editing. *Mamm. Genome* 28: 291–301. [Medline] [CrossRef]
3. Cao, X., Shores, E.W., Hu-Li, J., Anver, M.R., Kelsall, B.L., Russell, S.M., Drago, J., Noguchi, M., Grinberg, A., Bloom, E.T., Pau, L.W.E., Katz, S.I., Love, P.E. and Leonard, W.J. 1995. Defective lymphoid development in mice lacking expression of the common cytokine receptor gamma chain. *Immunity* 2: 223–238. [Medline] [CrossRef]
4. Cavazzana-Calvo, M., Hacein-Bey, S., de Saint Basile, G., Gross, F., Yvon, E., Nusbaum, P., Selz, F., Hue, C., Certain, S., Casanova, J.L., Bousso, P., Deist, F.L. and Fischer, A. 2000. Gene therapy of human severe combined immunodeficiency (SCID)-X1 disease. *Science* 288: 669–672. [Medline] [CrossRef]
5. Chang, C.W., Lai, Y.S., Westin, E., Khodadadi-Jamayran, A., Pawlik, K.M., Lamb, L.S. Jr., Goldman, F.D. and Townes, T.M. 2015. Modeling human severe combined immunodeficiency and correction by CRISPR/Cas9-enhanced gene targeting. *Cell Rep.* 12: 1668–1677. [Medline] [CrossRef]
6. Chen, D., Xu, T., Tu, M., Xu, J., Zhou, C., Cheng, L., Yang, R., Yang, T., Zheng, W., He, X., Deng, R., Ge, X., Li, J., Song, Z., Zhao, J. and Gu, F. 2018. Recapitulating X-Linked juvenile retinoschisis in mouse model by knock-in patient-specific novel mutation. *Front. Mol. Neurosci.* 10: 453. [Medline] [CrossRef]
7. Chen, S., Lee, B., Lee, A.Y., Modzelewski, A.J. and He, L. 2016. Highly efficient mouse genome editing by CRISPR ribonucleoprotein electroporation of zygotes. *J. Biol. Chem.* 291: 14457–14467. [Medline] [CrossRef]
8. Chen, S., Sun, S., Moonen, D., Lee, C., Lee, A.Y., Schaffer, D.V. and He, L. 2019. CRISPR-READI: Efficient generation of knockin mice by CRISPR RNP electroporation and AAV donor infection. *Cell Rep.* 27: 3780–3789.e4. [Medline] [CrossRef]
9. Cheng, C., Deng, P. Y., Ikeuchi, Y., Yuede, C., Li, D., Rensing, N., Huang, J., Baldridge, D., Maloney, S. E., Dougherty, J. D., Constantino, J., Jahani-Asl, A., Wong, M., Wozniak, D. F., Wang, T., Klyachko, V. A. and Bonni, A. 2018. Characterization of a mouse model of Borjeson-Forssman-Lehmann syndrome. *Cell Rep* 25: 1404–1414 e1406.
10. Darwish, M., Nishizono, H., Uosaki, H., Sawada, H., Sadahiro, T., Ieda, M. and Takao, K. 2019. Rapid and high-efficient generation of mutant mice using freeze-thawed embryos of the C57BL/6J strain. *J. Neurosci. Methods* 317: 149–156. [Medline] [CrossRef]
11. DiSanto, J.P., Müller, W., Guy-Grand, D., Fischer, A. and Rajewsky, K. 1995. Lymphoid development in mice with a targeted deletion of the interleukin 2 receptor gamma chain. *Proc. Natl. Acad. Sci. USA* 92: 377–381. [Medline] [CrossRef]
12. Goh, T.S., Jo, Y., Lee, B., Kim, G., Hwang, H., Ko, E., Kang, S.W., Oh, S.O., Baek, S.Y., Yoon, S., Lee, J.S. and Hong, C.

2017. IL-7 induces an epitope masking of gammac protein in IL-7 receptor signaling complex. *Mediators Inflamm.* 2017: 9096829. [Medline] [CrossRef]

13. Hacein-Bey-Abina, S., Hauer, J., Lim, A., Picard, C., Wang, G.P., Berry, C.C., Martinache, C., Rieux-Laucat, F., Latour, S., Belohradsky, B.H., Leiva, L., Sorensen, R., Debré, M., Casanova, J.L., Blanche, S., Durandy, A., Bushman, F.D., Fischer, A. and Cavazzana-Calvo, M. 2010. Efficacy of gene therapy for X-linked severe combined immunodeficiency. *N. Engl. J. Med.* 363: 355–364. [Medline] [CrossRef]

14. Hacein-Bey-Abina, S., Von Kalle, C., Schmidt, M., McCormack, M.P., Wulffraat, N., Leboulch, P., Lim, A., Osborne, C.S., Pawliuk, R., Morillon, E., Sorensen, R., Forster, A., Fraser, P., Cohen, J.I., de Saint Basile, G., Alexander, I., Wintergerst, U., Frebourg, T., Aurias, A., Stoppa-Lyonnet, D., Romana, S., Radford-Weiss, I., Gross, F., Valensi, F., Delabesse, E., Macintyre, E., Sigaux, F., Soulier, J., Leiva, L.E., Wissler, M., Prinz, C., Rabbitts, T.H., Le Deist, F., Fischer, A. and Cavazzana-Calvo, M. 2003. LMO2-associated clonal T cell proliferation in two patients after gene therapy for SCID-X1. *Science* 302: 415–419. [Medline] [CrossRef]

15. Hashimoto, M., and Takemoto, T. 2015. Electroporation enables the efficient mRNA delivery into the mouse zygotes and facilitates CRISPR/Cas9-based genome editing. *Sci. Rep.* 5: 11315. [Medline] [CrossRef]

16. Hashimoto, M., Yamashita, Y. and Takemoto, T. 2016. Electroporation of Cas9 protein/sgRNA into early pronuclear zygotes generates non-mosaic mutants in the mouse. *Dev. Biol.* 418: 1–9. [Medline] [CrossRef]

17. Hsu, P.D., Scott, D.A., Weinstein, J.A., Ran, F.A., Konermann, S., Agarwala, V., Li, Y., Fine, E.J., Wu, X., Shalem, O., Cradick, T.J., Marraffini, L.A., Bao, G. and Zhang, F. 2013. DNA targeting specificity of RNA-guided Cas9 nucleases. *Nat. Biotechnol.* 31: 827–832. [Medline] [CrossRef]

18. Inui, M., Miyado, M., Igarashi, M., Tamano, M., Kubo, A., Yamashita, S., Asahara, H., Fukami, M. and Takada, S. 2014. Rapid generation of mouse models with defined point mutations by the CRISPR/Cas9 system. *Sci. Rep.* 4: 5396. [Medline] [CrossRef]

19. Ito, M., Hiramatsu, H., Kobayashi, K., Suzue, K., Kawahata, M., Hioki, K., Ueyama, Y., Koyanagi, Y., Sugamura, K., Tsuji, K., Heike, T. and Nakahata, T. 2002. NOD/SCID/gamma(c) (null) mouse: an excellent recipient mouse model for engraftment of human cells. *Blood* 100: 3175–3182. [Medline] [CrossRef]

20. Kawahara, A., Minami, Y., Miyazaki, T., Ihle, J.N. and Taniguchi, T. 1995. Critical role of the interleukin 2 (IL-2) receptor gamma-chain-associated Jak3 in the IL-2-induced c-fos and c-myc, but not bcl-2, gene induction. *Proc. Natl. Acad. Sci. USA* 92: 8724–8728. [Medline] [CrossRef]

21. Kovanen, P.E., and Leonard, W.J. 2004. Cytokines and immunodeficiency diseases: critical roles of the gamma(c)-dependent cytokines interleukins 2, 4, 7, 9, 15, and 21, and their signaling pathways. *Immunol. Rev.* 202: 67–83. [Medline] [CrossRef]

22. Labun, K., Guo, X., Chavez, A., Church, G., Gagnon, J.A. and Valen, E. 2019. Accurate analysis of genuine CRISPR editing events with ampliCan. *Genome Res.* 29: 843–847. [Medline] [CrossRef]

23. Menon, T., Firth, A.L., Scripture-Adams, D.D., Galic, Z., Qualls, S.J., Gilmore, W.B., Ke, E., Singer, O., Anderson, L.S., Bornzin, A.R., Alexander, I.E., Zack, J.A. and Verma, I.M. 2015. Lymphoid regeneration from gene-corrected SCID-X1 subject-derived iPSCs. *Cell Stem Cell* 16: 367–372. [Medline] [CrossRef]

24. Morgulis, A., Gertz, E.M., Schäffer, A.A. and Agarwala, R. 2006. WindowMasker: window-based masker for sequenced genomes. *Bioinformatics* 22: 134–141. [Medline] [CrossRef]

25. Naito, Y., Hino, K., Bono, H. and Ui-Tei, K. 2015. CRISPRdirect: software for designing CRISPR/Cas guide RNA with reduced off-target sites. *Bioinformatics* 31: 1120–1123. [Medline] [CrossRef]

26. Nakade, S., Tsubota, T., Sakane, Y., Kume, S., Sakamoto, N., Obara, M., Daimon, T., Sezutsu, H., Yamamoto, T., Sakuma, T. and Suzuki, K.T. 2014. Microhomology-mediated end-joining-dependent integration of donor DNA in cells and animals using TALENs and CRISPR/Cas9. *Nat. Commun.* 5: 5560. [Medline] [CrossRef]

27. Ohbo, K., Suda, T., Hashiyama, M., Mantani, A., Ikebe, M., Miyakawa, K., Moriyama, M., Nakamura, M., Katsuki, M., Takahashi, K., Yamamura, K. and Sugamura, K. 1996. Modulation of hematopoiesis in mice with a truncated mutant of the interleukin-2 receptor gamma chain. *Blood* 87: 956–967. [Medline] [CrossRef]

28. Oliver, D., Yuan, S., McSwiggin, H. and Yan, W. 2015. Pervasive genotypic mosaicism in founder mice derived from genome editing through pronuclear injection. *PLoS One* 10: e0129457. [Medline] [CrossRef]

29. Puck, J.M., Pepper, A.E., Henthorn, P.S., Candotti, F., Isakov, J., Whitwam, T., Conley, M.E., Fischer, R.E., Rosenblatt, H.M., Small, T.N. and Buckley, R.H. 1997. Mutation analysis of IL2RG in human X-linked severe combined immunodeficiency. *Blood* 89: 1968–1977. [Medline]

30. Sharpe, J.J., and Cooper, T.A. 2017. Unexpected consequences: exon skipping caused by CRISPR-generated mutations. *Genome Biol.* 18: 109. [Medline] [CrossRef]

31. Smits, A.H., Ziebell, F., Joberty, G., Zinn, N., Mueller, W.F., Clauder-Münster, S., Eberhard, D., Fälth Savitski, M., Grandi, P., Jakob, P., Michon, A.M., Sun, H., Tessmer, K., Bürckstümmer, T., Bantscheff, M., Steinmetz, L.M., Drewes, G. and Huber, W. 2019. Biological plasticity rescues target activity in CRISPR knock outs. *Nat. Methods* 16: 1087–1093 [CrossRef]. [Medline]

32. Stemmer, M., Thumberger, T., Del Sol Keyer, M., Wittbrodt, J. and Mateo, J.L. 2015. CCTop: An intuitive, flexible and reliable CRISPR/Cas9 target prediction tool. *PLoS One* 10: e0124633. [Medline] [CrossRef]

33. Sunagawa, G.A., Sumiyama, K., Ukai-Tadenuma, M., Perrin, D., Fujishima, H., Ukai, H., Nishimura, O., Shi, S., Ohno, R.I., Narumi, R., Shimizu, Y., Tone, D., Ode, K.L., Kuraku, S. and Ueda, H.R. 2016. Mammalian reverse genetics without crossing reveals Nr3a as a short-sleeper gene. *Cell Rep.* 14: 662–677. [Medline] [CrossRef]

34. Xiao, A., Cheng, Z., Kong, L., Zhu, Z., Lin, S., Gao, G. and Zhang, B. 2014. CasOT: a genome-wide Cas9/gRNA off-target searching tool. *Bioinformatics* 30: 1180–1182. [Medline] [CrossRef]

35. Yang, H., Wang, H., Shivalila, C.S., Cheng, A.W., Shi, L. and Jaenisch, R. 2013. One-step generation of mice carrying reporter and conditional alleles by CRISPR/Cas-mediated genome engineering. *Cell* 154: 1370–1379. [Medline] [CrossRef]

36. Yoshimi, K., Kunihiro, Y., Kaneko, T., Nagahora, H., Voigt, B. and Mashimo, T. 2016. ssODN-mediated knock-in with CRISPR-Cas for large genomic regions in zygotes. *Nat. Commun.* 7: 10431. [Medline] [CrossRef]